American Mineralogist, Volume 77, pages 258–269, 1992

Raman and infrared study of pressure-induced structural changes in $MgSiO_3$, $CaMgSi_2O_6$, and $CaSiO_3$ glasses

J. D. KUBICKI*
Geophysical Laboratory and Center for High-Pressure Research, Carnegie Institution of Washington, Washington, DC 20015, U.S.A.

R. J. HEMLEY
Geophysical Laboratory and Center for High-Pressure Research, Carnegie Institution of Washington, Washington, DC 20015, U.S.A.,
and Department of Earth and Planetary Sciences, The Johns Hopkins University, Baltimore, Maryland 21218, U.S.A.

A. M. HOFMEISTER
Department of Geology, University of California, Davis, California 95616, U.S.A.

ABSTRACT

Raman and midinfrared spectra of $MgSiO_3$, $CaMgSi_2O_6$, and $CaSiO_3$ glasses have been measured to 45 GPa in a diamond cell. The principal pressure-induced changes in spectra observed are reversible, so that characterization of the high-density states of these materials requires in situ measurements at high pressure. The dominant change in all three glasses is a marked shift of the midfrequency Raman bands (at 625–650 cm^{-1}) to higher frequencies with increasing pressure. This indicates that the main compression mechanism is associated with a decrease in the average intertetrahedral Si-O-Si angles, as found in other silicate materials. The intensities of high-frequency Raman and infrared bands at 900–1200 cm^{-1} decrease with pressure relative to those of lower frequency bands. This is attributed to distortions of SiO_4 tetrahedra. However, the Raman and infrared spectra provide no direct evidence for a distinct $^{[4]}Si$ to $^{[6]}Si$ coordination change at room temperature in these glasses over the pressure range of this study. We present evidence that pressure-induced structural changes in glasses, including changes in cation coordination, can be affected by sample preparation and trace impurities.

INTRODUCTION

Information on the structure of molten silicates at very high pressures is essential for understanding and predicting the physical and chemical properties of deep-seated melts within the Earth. It is now recognized that the densities of basic to ultrabasic silicate melts at mantle pressures can approach those of crystalline phases with which they are in equilibrium (e.g., Rigden et al., 1984, 1988; Heinz and Jeanloz, 1987; Knittle and Jeanloz, 1989). This has important consequences for the formation of geochemical mantle reservoirs and planetary differentiation. The mechanism by which silicate melts can achieve high densities is incompletely understood. It is possible that the silicate liquids and glasses of these compositions undergo pressure-induced changes in cation coordination analogous to those documented for crystalline phases at high pressure (Waff, 1975; Matsui and Kawamura, 1980). These materials may also be compressed by angle bending in the Si-O-Si chains, which can maintain a bonding topology based on Si in tetrahedral coordination to high densities (Hemley and Kubicki, 1991). In addition, there may be topological rearrangements that preserve the basic $^{[4]}Si$ coordination. The relative contributions of these different compression mechanisms are expected to control the densities achieved in molten silicates in the Earth's mantle.

Raman scattering and infrared absorption spectroscopy have been particularly useful for obtaining structural information on silicate glasses (e.g., Hibben, 1935), leading to insights into the properties of melts at higher temperatures. In recent years, these techniques have provided a wealth of spectral information on the short- and intermediate-range structure of these glasses (Sweet and White, 1969; Brawer and White, 1977; Mysen et al., 1980; McMillan, 1984a, 1989). One of the advantages of Raman and infrared techniques relative to other methods (Wong and Angell, 1976; Cusack, 1987) is the possibility of using them in high-pressure studies with the diamond cell (Jayaraman, 1983; Hemley et al., 1987; Mao, 1989). As a result, structural changes in silicate glasses under deep Earth conditions can be examined without recourse to

* Present address: Division of Geological and Planetary Sciences, California Institute of Technology, Pasadena, California 91125, U.S.A.

0003–004X/92/0304–0258$02.00

pressure quenching, which may not yield structural states that are representative of the high-pressure form of the glass.

Vibrational spectroscopic measurements on silicate glasses at high pressure in the diamond cell document that significant changes in local structure occur above 10 GPa (e.g., Hemley et al., 1986; Williams and Jeanloz, 1988). The results indicate that large distortions of SiO_4 tetrahedra, and possibly an increase in Si coordination, occur at high pressure and room temperature in silicate glasses. Furthermore, the principal spectral changes induced by pressure are reversible and thus require in situ high-pressure measurements to be observed (Hemley et al., 1986; Williams and Jeanloz, 1988). There is a need to examine this behavior for a variety of chemical compositions relevant to the lower mantle. These high-pressure, vibrational spectra provide information on possible short- and intermediate-range order in calcium magnesium metasilicate glasses under very high compression and may be used to infer the structure of silicate melts in the mantle.

In the present study, in situ Raman and midinfrared spectroscopic measurements of $MgSiO_3$ (enstatite), $CaMgSi_2O_6$ (diopside), and $CaSiO_3$ (wollastonite) glasses were made to lower mantle pressures. $MgSiO_3$ perovskite is thought to be the dominant end-member phase in the lower mantle (Liu, 1975; Yagi et al., 1978), and $CaSiO_3$ perovskite may be a secondary constituent (Liu and Ringwood, 1975; Mao et al., 1989). An investigation of the vitreous state of these compositions provides a starting point for understanding the structure of mantle melts. Substitution of Ca for Mg is also used to clarify the role of the network-modifying cations of the structure in the glasses. Because Raman and infrared spectroscopies detect different vibrational modes in the material, the use of both provides complementary information on the vibrations in the glass that can be related to the high-pressure structure. These measurements are also compared with results from molecular dynamics simulations of compression in $MgSiO_3$ glass and melt.

Experimental methods

Glasses were prepared in our laboratory from spectroscopic-grade oxide and carbonate powders mixed in an agate mortar and pestle under ethanol for 15 min. The samples were then decarbonated at 1000 °C for over 4 h. Sintered samples were melted in a Pt-wound furnace at least 25 °C above the melting point for 1 h in a Pt capsule with 5-mm diameter, quenched in H_2O, ground, and remelted. Each sample was analyzed optically to ensure that the glasses were free of crystallites. Compositions were measured by electron microprobe to confirm the stoichiometries and were within ±0.2 wt% of the ideal compositions. A small amount of grinding in an agate mortar and pestle was necessary to ensure that grain sizes of less than 10 μm were available for the diamond cell. We also measured Raman spectra of two $MgSiO_3$ glasses prepared independently at 1620 °C (by H. S. Yoder) and 1650 °C (by J. Bass) and quenched in H_2O at 0.1 MPa (1 bar). Another $MgSiO_3$ glass, quenched at 0.2 GPa and 1650 °C in a piston-cylinder apparatus (by F. R. Boyd and J. England) at the Geophysical Laboratory, was used in the Raman experiments. All samples used for the high-pressure experiments were free of crystallites, as determined by optical microscopy and Raman spectroscopy.

Samples were compressed in megabar-type Mao-Bell diamond-anvil cells using T-301 stainless steel gaskets preindented to 10–20 GPa (Mao, 1989). No pressure-transmitting media were used in most experiments in order to achieve the strongest possible signal. This was important because of the very low Raman scattering cross section of these glasses (particularly $MgSiO_3$). Selective measurements were performed on samples compressed in Ar pressure-transmitting media to examine effects of nonhydrostatic stress (e.g., Hemley et al., 1986, 1987). Pressure measurements were made with the standard ruby method (Mao et al., 1986). Precision was within ±0.1 GPa on any given ruby grain in the sample. Six separate pressure measurements were made for each spectrum to determine the pressure variation in the sample. With ruby dispersed throughout the sample, pressures were measured on a grid of points over the entire gasket opening and averaged to obtain the quoted sample pressure. Standard deviations in the pressure measurements across the sample were approximately 10% of the average pressure at the maximum loads.

Raman spectra were measured with a micro-optical system designed for diamond-cell samples with weak Raman scattering cross sections (Hemley et al., 1986, 1987). The spectrometer consisted of a triple spectrograph (Spex Triplemate) and intensified diode-array detector (optical-multichannel analyzer, Princeton Instruments). A window of 55 nm typically centered at 539.5 nm was used. Raman spectra were excited with the 514.5-nm line of an Ar^+ laser (Spectra Physics model 165) at a power of 5–50 mW focused to a diameter of ≈3–10 μm. An aperture giving a sampling area of approximately 5 × 10 μm was used to discriminate against background signal from the diamond anvils (Hemley et al., 1987). Spectra were typically signal averaged from ½ to 1 h. Resolution of the spectra was approximately 10 cm^{-1} with a grating of 600 grooves/mm. Overlapping bands in the several sets of spectra were curve fitted with Voight profiles using least-squares techniques.

Samples for the infrared measurements were prepared by crushing the sample between the diamond anvils into a platelet of 1–2 μm thickness (Hofmeister et al., 1989). A layer of CsI was placed on top of the sample, and dispersed ruby grains were added for pressure calibration. The infrared absorption spectra were measured over the total sample area (i.e., diameter ~200 μm), whereas individual Raman measurements were made on small portions of the sample (i.e., <10 μm). Infrared spectra were measured on a Nicolet 7199 FT-IR spectrometer with a liquid N_2–cooled HgCdTe detector and a custom-designed beam condenser (Hofmeister et al., 1989). Three

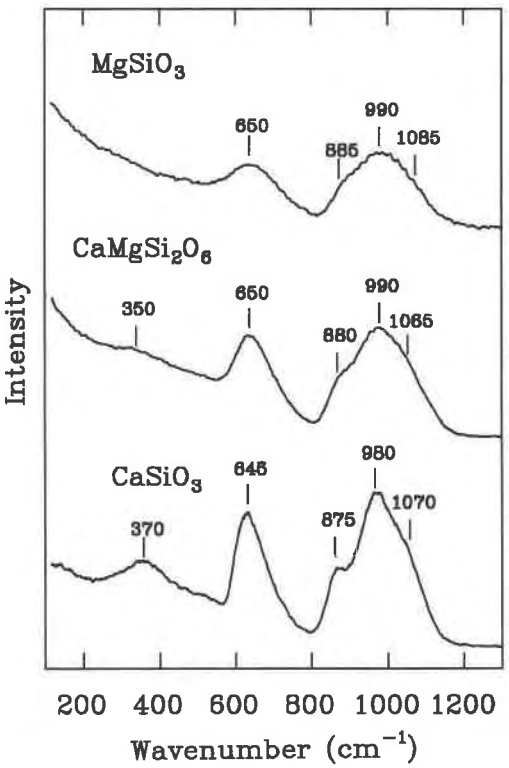

Fig. 1. Raman spectra of $MgSiO_3$, $CaMgSi_2O_6$, and $CaSiO_3$ glasses at 0.1 MPa (1 bar, 300 K). Spectra were measured on diamond-cell sized samples with the micro-Raman spectrometer prior to compression.

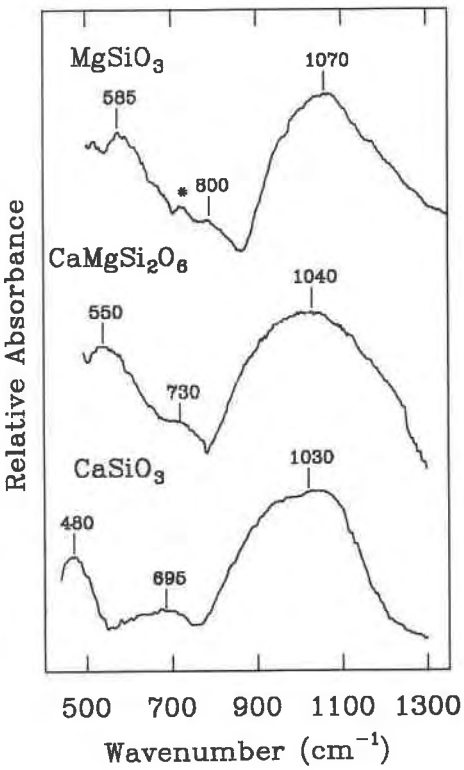

Fig. 2. Mid-infrared absorption spectra of $MgSiO_3$, $CaMgSi_2O_6$, and $CaSiO_3$ glasses measured at low pressures (<2 GPa) in a diamond-anvil cell under nominal load (300 K). The asterisk denotes a peak due to ruby used for pressure calibration.

sets of 4000 scans were averaged for each spectrum, which had a resolution of 2 cm^{-1}. Background spectra were recorded using an empty diamond cell.

Results

Ambient pressure spectra

Ambient pressure (0.1 MPa) Raman spectra of the samples are presented in Figure 1. Peak positions of the low- and midfrequency bands agree with previously measured spectra to within ± 2 cm^{-1} (Mysen et al., 1982; McMillan, 1984b). No temperature effects related to sample preparation were apparent in the 0.1 MPa spectra (within the present experimental resolution). However, the high-pressure response of an $MgSiO_3$ sample prepared in a piston-cylinder apparatus at 0.2 GPa differed markedly from that of samples quenched at ambient pressure, as will be discussed below. The spectra of $CaSiO_3$ and $CaMgSi_2O_6$ have broad bands at 350–370 cm^{-1}. The intensities of these bands increase with Ca content. In all three compositions, a band of intermediate relative intensity is observed between 600 and 700 cm^{-1} at ambient pressure. This peak has an asymmetric line shape, particularly in the spectrum of $CaSiO_3$ and is broadest in the $CaMgSi_2O_6$ composition. A band from 800 to 1200 cm^{-1} is observed in all three spectra, with shoulders flanking the most intense peak at approximately 900 and 1100 cm^{-1}. The shoulders are more highly resolved from the main band for $CaSiO_3$ in comparison with the other two compositions. Mysen et al. (1982) and McMillan (1984b) have shown that this high-frequency band may be fitted with contributions from five peaks at 870, 915, 970, 1060, and 1150 cm^{-1}.

Midinfrared spectra of the glasses at low pressure are shown in Figure 2. The spectra are similar and consist of three broad bands at 400–600, 600–800, and 800–1250 cm^{-1}. All three bands shift to higher frequency with increasing Mg content of the glass. This shift is most pronounced in the lowest frequency band, which varied from 480 cm^{-1} in $CaSiO_3$ to 585 cm^{-1} in $MgSiO_3$ glass. The spectrum of the glasses at low pressure is similar to those reported previously (Williams and Jeanloz, 1988).

High-pressure spectra

In situ, high-pressure Raman spectra are presented in Figure 3. The Raman scattering cross sections of these glasses are low, but spectral peaks are well above the background signal from the diamond cell to pressures above 30 GPa. The high-pressure spectra reveal large pressure effects on several bands. The largest changes observed occur in the 645–650 cm^{-1} bands (0.1-MPa frequencies). The positions of these bands shift linearly with pressure up to at least ~30 GPa. Above this pressure, the

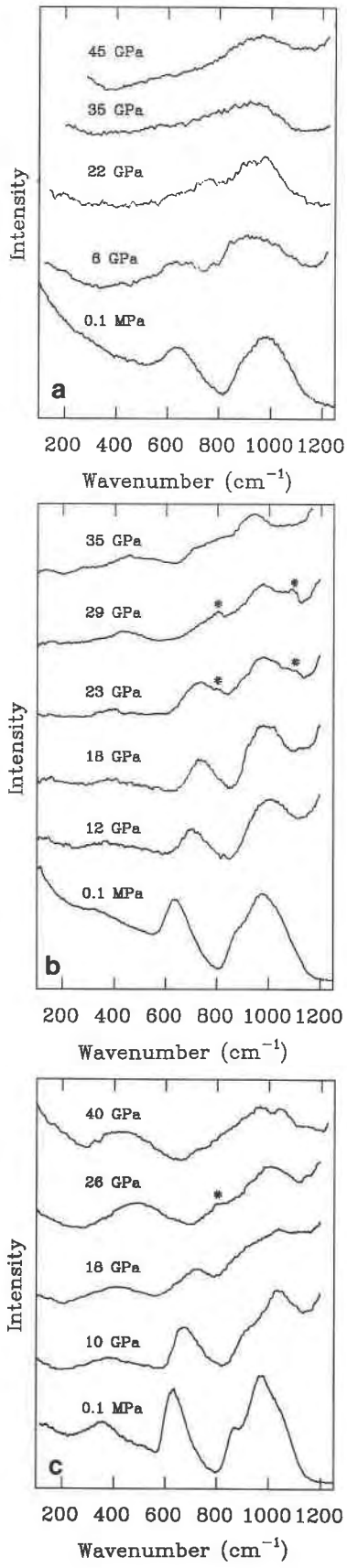

peaks merge with the high-frequency bands and cannot be traced to higher pressure. The low-frequency Raman bands observed in $CaSiO_3$ and $CaMgSi_2O_6$ (350 and 370 cm^{-1}) have weaker, positive pressure shifts. In addition, a decrease in the broad scattering intensity at low frequency (<600 cm^{-1}) is observed initially with increasing pressure. Weak shifts in the positions of the low-frequency bands and relative intensities are observed above 20 GPa (particularly in $CaMgSi_2O_6$ and $CaSiO_3$). The pressure dependence of the high-frequency bands at 850–1100 cm^{-1} are slight but weakly negative in $MgSiO_3$ and $CaMgSi_2O_6$. This effect partially arises from the increase in relative intensity of the lower frequency (860–885 cm^{-1}) components. This is borne out by preliminary curve fitting of the high-frequency bands as a function of pressure. Notably, the structure of the high-frequency envelope changes with pressure, which indicates that polymerization of the SiO_4 tetrahedra is altered even at low pressures (and 300 K). This is particularly marked in $CaSiO_3$ glass.

High-pressure Raman spectra were similar for glasses obtained from different sources (within experimental uncertainty). An important exception was the $MgSiO_3$ glass sample synthesized 0.2 GPa. The evolution of the spectra measured for this sample with increasing pressure is shown in Figure 4. The spectra were similar to those measured for other samples up to approximately 25 GPa. At higher pressures, however, a new band at approximately 400 cm^{-1} was observed (Kubicki and Hemley, 1988). This peak appeared reproducibly in this pressure range in three separate experiments with this glass sample (two experiments with no pressure-transmitting medium and one with an Ar medium). With increasing pressure, the intensity of the new peak increased and the bandwidth decreased. Upon decompression, the peak diminished in intensity but remained detectable to 18 GPa. Similar results were obtained both with and without an Ar medium, indicating that shear stresses have only a small effect on the high-pressure spectral changes. Spectra measured up to 45 GPa on the other samples of $MgSiO_3$ glass did not show this feature (see below).

Midinfrared spectra of the three glasses are shown in Figure 5. Changes in the spectra are continuous from 0.1 MPa to 25 GPa. Low-frequency infrared band shifts are small (0.8–1.2 cm^{-1}/GPa) in all three samples. All three

←

Fig. 3. High-pressure Raman spectra of (**a**) $MgSiO_3$ (glass A) (**b**) $CaMgSi_2O_6$, and (**c**) $CaSiO_3$ glasses from 0.1 MPa to 35–45 GPa measured in the diamond cell (300 K). Measurements of pressure from different ruby grains embedded in the samples indicate that the variation in pressure across each sample is less than 10% of the average pressure. However, the pressure variation across the portion of the sample probed by the laser for each measurement is estimated to be of order 1% (neglecting possible uniaxial stresses, which are unknown). The asterisks denote extraneous Raman or fluorescence bands. The rise in intensity above 1200 cm^{-1} is due to the strong T_{2g} band of the diamond anvil (peak position of 1333 cm^{-1} at 0.1 MPa).

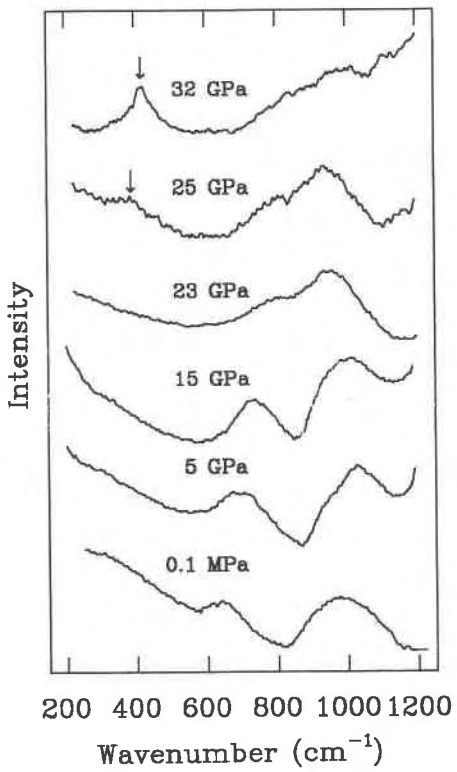

Fig. 4. Raman spectra of $MgSiO_3$ glass prepared by Boyd and England under 0.2 GPa pressure in a piston-cylinder (glass B). The high-pressure peak near 400 cm^{-1} is identified by arrows in the two highest pressure spectra. The spectral changes with pressure are reversible but exhibited hysteresis on decompression. The peak positions and relative intensities of the spectra below 25 GPa are similar to those observed in the other $MgSiO_3$ glass samples (Fig. 3a). A larger amount of low-frequency scatter was observed at 0.1 MPa as a result of the lower optical quality of the starting sample, but the sample appeared homogeneous by optical microscopy.

bands also decrease in absorbance with pressure. A second low-frequency mode (~580 cm^{-1}) in $MgSiO_3$ and $CaMgSi_2O_6$ glasses shifts at 4.4 (± 0.1) cm^{-1}/GPa. Midfrequency infrared modes in $MgSiO_3$ and $CaMgSi_2O_6$ (800 and 730 cm^{-1}, respectively) decrease in frequency with pressure. In $CaSiO_3$ glass, the frequency of the 710-cm^{-1} band is nearly independent of pressure. A gradual decrease in absorbance between 900 and 1250 cm^{-1} occurs in each glass, and the region becomes flat with respect to the background above 35 GPa. The high-frequency band broadens and decreases in absolute and relative intensity with increasing pressure. In each case, the frequencies shift linearly with pressure (within experimental uncertainty). The high-pressure infrared spectra of $CaMgSi_2O_6$ glass are comparable to that reported by Williams and Jeanloz (1988), although there appears to be some differences that are likely associated with differences in the method of sample preparation and loading (cf. Hofmeister et al., 1989).

Discussion

One of the key observations of the present study is the large difference between spectra measured at ambient and high pressures (e.g., above ~10 GPa), particularly in the Raman measurements. The changes induced by pressure greatly exceed the differences due to Mg-Ca substitution and differences in spectra measured at 0.1 MPa before and after pressure cycling. In general, the bands become weaker with pressure, partly as a result of sample thinning. However, the low-frequency infrared bands are less affected and, in some cases, become stronger with pressure. In contrast, the higher frequency bands markedly decrease in intensity with pressure. The intensity of the broad, low-frequency (<500 cm^{-1}) Raman features initially decreases with increasing pressure. Generally, the vibrational bands have positive frequency shifts with pressure, though midfrequency infrared bands are an exception. The compositional effect on the magnitude of these shifts appears slight.

The results indicate that significant changes in structure occur in these glasses under pressures at room temperature. Although a quantitative interpretation of spectral changes requires calculation of the optical response of the glasses from accurate structural models, the observed frequency shifts can be understood at a qualitative level in terms of possible changes in bond lengths, bond angles, and cation coordination with pressure. We begin such an analysis with an examination of vibrational band assignments and the available information on the structure of the glasses under ambient conditions.

Vibrational band assignments

The low-, mid-, and high-frequency bands have been associated with Ca and Mg coordination polyhedra, Si-O-Si tetrahedral linkages, and SiO_4 tetrahedra, respectively. Etchepare (1972) has associated peaks in the frequency range of 300–400 cm^{-1} with Ca and Mg in octahedral coordination based on comparisons between glass and crystal spectra. Eckersley et al. (1988a, 1988b) report evidence from EXAFS and neutron-scattering experiments that Ca has well-defined octahedral coordination in $CaSiO_3$ glass. Analysis of X-ray diffraction results by Yin et al. (1983) indicates that each Mg ion is surrounded by four O ions at 2.08 Å and two more at 2.50 Å (see also Waseda and Toguri, 1977). Hanada et al. (1988) also conclude from X-ray emission spectra that Mg is in fourfold coordination in amorphous $MgSiO_3$ films. As discussed below, molecular dynamics (MD) simulations (Matsui et al., 1981; Kubicki and Lasaga, 1987, 1991) predict that Mg coordination is ill-defined in $MgSiO_3$ glass and ranges from tetrahedral to octahedral. The Raman intensity of the low-frequency peak also decreases from $CaSiO_3$ to $MgSiO_3$ in these glasses. These observations may be taken as evidence for a decreasing concentration of network-modifying cations in octahedral coordination with increasing Mg content (e.g., Navrotsky et al., 1985).

Midfrequency Raman bands (600–700 cm^{-1}) of a va-

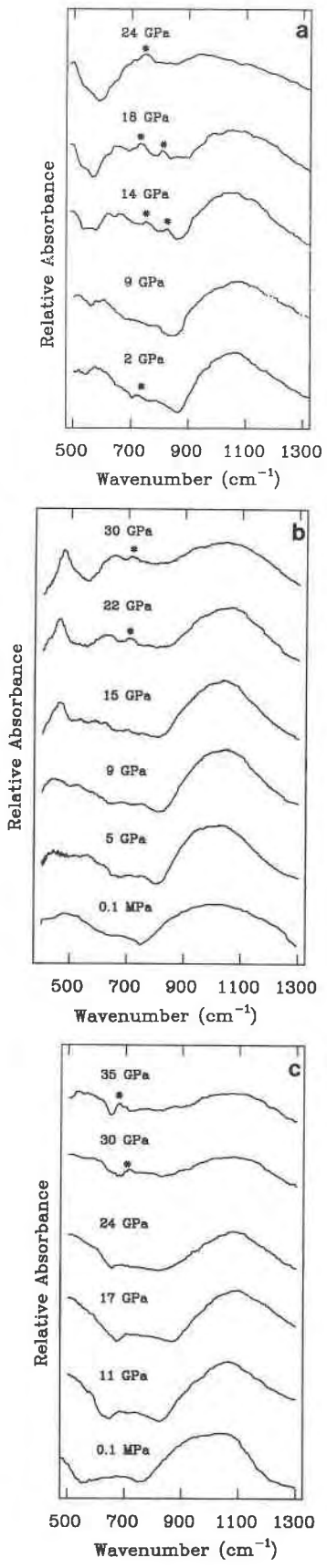

riety of metasilicate glasses have been assigned to vibrational modes characteristic of Si-O-Si intertetrahedral linkages (Furukawa et al., 1981; Matson et al., 1983; McMillan, 1984a). Specifically, these studies indicate that a mode with contributions from bridging O symmetric stretching and Si-O-Si angle bending gives rise to the Raman intensity at this frequency. The high-frequency band has been deconvoluted into five peaks associated with symmetric stretches of Si-O bonds in different polymerized species of Si tetrahedra [i.e., Q^0–Q^4, where the superscript denotes the number of bridging O atoms in the SiO_4 tetrahedra (McMillan, 1984b)]. By this analysis, intensities of the individual contributions to this band are related to the polymerization state of the sample.

Infrared bands in the low-frequency region (below 600 cm^{-1}) have been attributed to combinations of O-Si-O bending modes with Si in tetrahedral coordination (Moenke, 1974). A mode of asymmetric Si-O-Si angle bending and bridging O asymmetric stretching vibrations causes the midfrequency absorption. High-frequency bands in the midinfrared have been assigned to asymmetric Si-O stretching modes in SiO_4 tetrahedra (e.g., Velde and Couty, 1987; Dowty, 1987).

Principal compression mechanisms

The largest effect of pressure is observed for the midfrequency Raman bands at 600–700 cm^{-1}. The pressure shift for these bands is generally linear, with large positive $d\nu_i/dP$ of 5–6 cm^{-1}/GPa. This frequency region has been assigned to modes associated with bridging O stretches, with some contributions from Si-O-Si angle bending (Furukawa et al., 1981; Matson et al., 1983; McMillan et al., 1989). Furukawa et al. (1981) studied the relationship between the intertetrahedral angle and vibrational frequency for a mixed mode of bridging O stretching and Si-O-Si angle bending in model Si_2O_6 chain units. Their results showed an inverse relationship between vibrational frequencies and Si-O-Si angles. Decreasing the Si-O-Si angle from 180° to 105° increased the calculated vibrational frequency from 490 to 650 cm^{-1}. Molecular orbital calculations on $H_6Si_2O_7$ (Lasaga and Gibbs, 1987, 1988) show that the curvature of the potential well rises steeply for an intertetrahedral angle below 140°. This increase in curvature causes an increase in the associated vibrational frequency. Hence, the observed behavior in the glass spectra indicates that the average intertetrahedral angles decrease appreciably with pressure.

The inverse relationship between the intertetrahedral

←

Fig. 5. High-pressure midinfrared absorption spectra of (**a**) $MgSiO_3$, (**b**) $CaMgSi_2O_6$, and (**c**) $CaSiO_3$ glasses up to at least 24 GPa measured in the diamond-anvil cell (300 K). In each case the standard deviation in pressure is approximately 10% of the total average pressure. Peaks marked with asterisks are from ruby grains used for pressure calibration.

TABLE 1. Si and Mg ion coordination as a function of density for an $MgSiO_3$ glass at 300 K from the molecular dynamics simulations*

Density (g/cm³)	Pressure** (GPa)	Cation	Cation coordination number (%)†				
			4	5	6	7	8
2.54	−6.0	Si^{4+}	99.0	1.0	0.0	0.0	0.0
		Mg^{2+}	66.3	28.6	5.1	0.0	0.0
2.75	0.0	Si^{4+}	100.0	0.0	0.0	0.0	0.0
		Mg^{2+}	67.4	30.2	4.7	0.5	0.0
3.00	9.0	Si^{4+}	96.0	4.0	0.0	0.0	0.0
		Mg^{2+}	27.5	42.1	27.7	1.9	0.0
3.40	29.0	Si^{4+}	91.2	8.0	0.0	0.0	0.0
		Mg^{2+}	5.7	34.0	44.5	14.5	1.3
3.88	60.0	Si^{4+}	72.8	26.6	0.6	0.0	0.0
		Mg^{2+}	0.0	12.2	42.8	38.1	6.9
4.25	93.0	Si^{4+}	34.5	51.1	14.4	0.0	0.0
		Mg^{2+}	0.0	1.1	19.3	42.9	36.6

* Kubicki and Lasaga (1991).

** Densities at a given pressure are calculated from a second-order Birch-Murnaghan equation of state for $MgSiO_3$ glass with $K_0 = 88$ GPa ($K_0' = 4$ assumed) and an experimental ambient pressure density of 2.75 g/cm³ (Yoder, 1976; J. Bass, unpublished data).

† Coordination numbers defined with maximum bond distances of 2.0 and 2.8 Å for Si-O and Mg-O bonds, respectively.

angles and the frequency of the symmetric Si-O-Si stretching mode in SiO_2 polymorphs was pointed out by Sharma et al. (1981). Matson et al. (1983) observed systematic shifts in frequencies of midfrequency peaks in glasses of other compositions and connected the changes in the average intertetrahedral angle. They noted that the average Si-O-Si angle in crystalline lithium disilicate sheets is 137° and for α sodium disilicate it is 149.5°. A corresponding increase in the frequency of the 500-cm^{-1} peak also occurs in the spectra of glasses of the same compositions. In addition, Sharma et al. (1981) and Matson et al. (1983) noted that the frequency of the Si-O-Si symmetric stretching mode in silicates with four-membered Si rings occurs above 500 cm^{-1}, whereas in those with six-membered rings, the frequency is 480 cm^{-1}; this is consistent with the inverse correlation between the average Si-O-Si angle and ring size.

The compression of many polymerized silicate minerals has been found to take place mainly by the closure of Si-O-Si angles (Levien et al., 1980; Hemley, 1987; Hazen et al., 1989). Quantitative methods for determining average Si-O-Si angles (e.g., by X-ray techniques) have not yet been developed for glasses at high pressures. Hence, it is useful to compare vibrational spectra of the glasses with those of crystalline silicates where bond angles have been determined by X-ray diffraction. The studies of crystalline silicates suggest that the position of the midfrequency peak is a function of mean Si-O-Si angle. The most probable explanation for the shift in the midfrequency peaks observed in this study is that the Si-O-Si angles decrease with pressure and this increases the frequency of the associated vibrational mode.

Comparison of the high-pressure vibrational spectra with the results of recent molecular dynamics (MD) simulations provides additional insight into the mechanism of compression. MD simulations carried out with potentials derived from molecular orbital theory (Lasaga and Gibbs, 1987) and electron-gas calculations (Cohen and Gordon, 1976) have shown that the closure of the Si-O-Si angle is linear with pressure up to a volume compression (V/V_0) of ~0.50, where V_0 is the volume at 0.1 MPa (Kubicki and Lasaga, 1987). MD calculations predict that the average Si-O-Si angle decreases from 147° to 132° for a density increase from 2.75 to 3.40 g/cm³, which corresponds to $V/V_0 = 0.8$. The reduction of the Si-O-Si angle at 30 GPa from the MD simulations is 15° or −0.5°/GPa. According to the calculations of Furukawa et al. (1981), a reduction of the Si-O-Si angle by 15° should shift the band by 60 cm^{-1}. This is in qualitative agreement with the observed shift. From the experimentally determined bulk modulus of $MgSiO_3$ glass we estimate $V/V_0 = 0.8$ at 30 GPa (Table 1).

Another important observation is the decrease in diffuse Raman scattering intensity at low frequencies (<500 cm^{-1}) with initial increase in pressure (<10 GPa; Fig. 3). Similar changes occur in SiO_2 glass, where the effect is even more pronounced (Hemley et al., 1986). The change in the SiO_2 spectra is likely due to a decrease in the intertetrahedral angle distribution, which results in an increase in intermediate-range order in the glass over this pressure range (Hemley et al., 1986). Similar effects are likely in the present metasilicate glasses. The weak low-frequency bands in the Raman spectra of $CaSiO_3$ and $CaMgSi_2O_6$ glasses have positive shifts with pressure. These bands have been assigned to motions of Ca in octahedral coordination. Hence, the pressure shifts in these bands indicate a mode of compression involving a decrease in the average Ca-O bond length. No evidence was observed of a change in Ca cation coordination. This behavior is consistent with the high compressibility of Ca-O bonds in crystalline materials (Hazen and Finger, 1982). We suggest that the 360-cm^{-1} band appears in spectra of glasses with Ca in regular octahedral coordination (Eckersley et al., 1988a, 1988b) and not in low-pressure $MgSiO_3$ glass spectra because the coordination state of Mg is irregular and is closer to tetrahedral than octahedral coordination (Yin et al., 1983). The effect of pressure may be to increase the regularity of the coordination polyhedra of the Mg (see below).

Finally, high-frequency bands in both the Raman and infrared spectra decrease in relative and absolute intensity with pressure in each of the glasses studied. However, the Raman bands in this frequency range have appreciable intensity up to 45 GPa, which indicates that SiO_4 tetrahedra are present in these glasses at least to this pressure. The observed intensity loss may be related to distortions in the tetrahedra (Hemley et al., 1986) and sample thinning with pressure. Within the high-frequency band, an increase in relative intensity of the 900-cm^{-1} shoulder is observed. This implies that the population of Q^1 species (one bridging O atom) associated with this band may increase with pressure. Xue et al. (1989) and Dickinson et al. (1990) present evidence that pressure

favors the disproportionation reaction $2Q^3 \rightleftharpoons Q^2 + Q^4$ in alkali silicates. The analogous reaction, $2Q^2 \rightleftharpoons Q^1 + Q^3$, may occur under pressure in the present metasilicate glasses. However, Wolf et al. (1990) do not find evidence for this reaction occurring on compression. There may also be contribution to the 900-cm^{-1} band from a small concentration of $^{[5]}Si$ (McMillan et al., 1989; Kubicki and Lasaga, 1991). The evidence for a discrete coordination change of Si is examined in detail below.

Reversibility of spectral changes

The gross spectral changes that occurred under pressure are fully reversible upon decompression. There are, however, minor differences between the ambient pressure spectra measured before and after compression. Decompressed sample peak positions are within ± 10 cm^{-1} (generally much closer) of the original positions at 0.1 MPa. For example, after pressure cycling to 32 GPa, the position of the broad midfrequency peak in the Raman spectrum of $MgSiO_3$ glass changes from 651 to 647 cm^{-1}, and the bandwidth (full-width at half-maximum, FWHM) decreases slightly from 134 to 113 cm^{-1}. Another change is the increase in intensity of the shoulder at 885 cm^{-1} relative to the 650-cm^{-1} band in this glass following decompression. These small differences in peak positions and widths suggest that there may be a small degree of densification (irreversible compaction) of these glasses upon room-temperature compression on the time scales (hours to days) and over the pressure range (30–45 GPa) of these experiments. However, the spectral changes are small in comparison with the large scale changes observed in the spectra measured in situ at high pressure.

Walrafen and Krishnan (1981) studied the Raman spectra of SiO_2 glass compacted at 9 GPa and 23 °C and found minor shifts in the high-frequency bands. These authors noted a 5–13-cm^{-1} frequency increase and 18-cm^{-1} narrowing of the 440-cm^{-1} band in the compacted glass. Seifert et al. (1983) measured Raman spectra of SiO_2 glass annealed at 900 °C up to 2 GPa and found changes of 10 cm^{-1} samples densified up to 7%. McMillan et al. (1984) observed much larger spectral shifts in SiO_2 glass densified at 3.95 GPa and 530 °C, as the sample was compressed approximately 6% above the normal density. Raman spectra obtained by McMillan et al. (1984) had shifts of 50 and 40 cm^{-1} in the two high-frequency peaks, and the band near 430 cm^{-1} in the normal glass increased to 470 cm^{-1} with an accompanying 50% decrease in peak width. Hemley et al. (1986) produced a pressure-quenched SiO_2 glass at ambient temperature with a Raman spectrum markedly different from the 0.1-MPa spectra. The strongest band shifted from 440 to 520 cm^{-1}, and the high-frequency bands shifted from 800 and 1060 cm^{-1} to 815 and 1000 cm^{-1}, respectively. These shifts are of similar magnitude to those induced with high-temperature annealing at pressure, but the maximum pressure in the low-temperature compression was over 30 GPa compared with 4 GPa in the McMillan et al. (1984) study. In view of the evidence that significant frequency shifts accompany densification (Seifert et al., 1983; McMillan et al., 1984), it is unlikely that a sizable increase in density (i.e., >5%) could be accomplished in these glasses without inducing structural changes observable with vibrational spectroscopy. We suggest that the small differences between the spectra of the starting material and decompressed samples indicate that the densification of these glasses is small in these room-temperature experiments (e.g., in comparison to that observed for SiO_2). This needs to be examined by direct measurements of the degree of densification, which will likely require larger samples than those studied here.

Evidence for structural transformations

As discussed above, changes in the low-frequency Raman spectra of the glasses are observed at pressures above ~20 GPa. This behavior was most pronounced in spectra of the magnesium silicate glass sample quenched in a piston-cylinder apparatus above 25 GPa (glass B). A relatively sharp peak near 400 cm^{-1} appeared, which increased in relative intensity and decreased in bandwidth with further increase in pressure. The changes were reversible but accompanied by hysteresis. Upon decompression, the peak diminished in intensity but remained detectable to 18 GPa. The peak was observed in three separate experiments on this sample, including an experiment carried out with Ar as a pressure-transmitting medium. Unfortunately, this sample had been consumed before this difference with subsequently prepared samples was detected; infrared measurements were not made on this glass sample.

We attribute the changes in the low-frequency Raman spectra at high pressure to a structural transition in the glass. It is unlikely that the transition is associated with crystallization (e.g., Hemley et al., 1989a) because of the reversible changes in the spectra (i.e., disappearance of the peak on decompression). In addition, no other crystal-like peaks are observed in the high-pressure state, and the band is broad relative to those measured for crystalline phases (see below). We also consider the possibility of disproportionation of $MgSiO_3$. There is some evidence for this reaction in $MgSiO_3$ glass samples that have been melted in situ at 30 GPa with a Nd-YAG laser (Kubicki and Hemley, 1989). Raman spectra of such samples, however, are distinct from those observed here. Further, the reversibility of the spectra on decreasing pressure suggests that no disproportionation of $MgSiO_3$ (e.g., to MgO and SiO_2) has taken place. Such a reaction would require chemical diffusion, which is slow at room temperature compared with the time scale of these experiments.

The difference in the high-pressure spectra may be affected by differences in sample preparation (especially the quench pressure). There is evidence that differences in quench rates can affect glass structure in SiO_2 (Galeener and Geissberger, 1983; Grimsditch, 1986) and $CaMgSi_2O_6$ (Brandriss and Stebbins, 1988), and variations in thermodynamic properties have been observed in calcium magnesium metasilicate glasses with different ther-

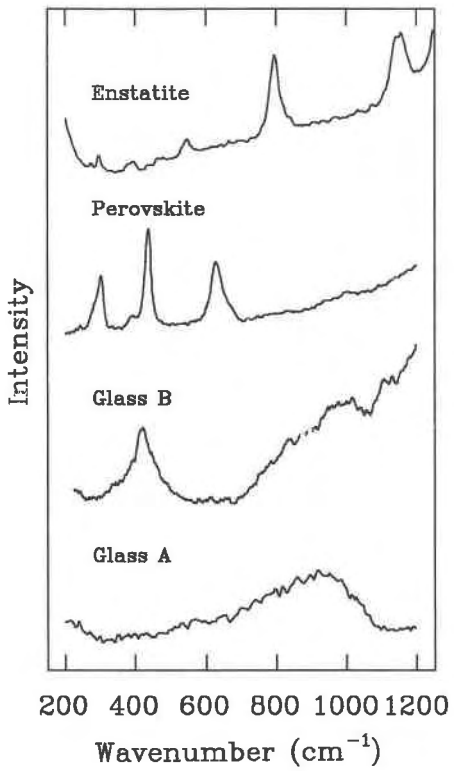

Fig. 6. Comparison of high-pressure Raman spectra of two magnesium silicate glasses, enstatite, and $MgSiO_3$ perovskite. The spectra of glass A and B were measured at 35 and 32 GPa, respectively. The spectra of orthoenstatite and $MgSiO_3$ perovskite were measured at 30 GPa and 22 GPa (Kubicki and Hemley, unpublished data; Hemley et al., 1989b). The frequency shift with pressure for the band at 430 cm^{-1} in the perovskite phase is 2.4 (± 0.1) cm^{-1}/GPa (Hemley et al., 1989b), so its frequency would increase by approximately 24 cm^{-1} from 22 to 32 GPa. The intensities are relative; the Raman scattering cross sections for orthoenstatite and perovskite spectra are approximately an order of magnitude and a factor of 2 greater than those of the glass spectra, respectively. The sloping base line in the glass B spectrum arises from residual diamond-anvil fluorescence.

mal histories (Richet and Bottinga, 1986). Although the ambient pressure spectra of the $MgSiO_3$ samples were indistinguishable, we suggest that small differences at 0.1 MPa are amplified by the effects of pressure. The behavior could also arise from impurities (e.g., H_2O), annealing, and storage conditions. Our Raman measurements showed no sign of H_2O, but the presence of very small amounts of H_2O (bound as OH) in the material could be responsible for this behavior. The kinetics of high-pressure transformations in glasses are strongly dependent on trace impurities (e.g., Fratello et al., 1981). Trace amounts of impurities such as H_2O are known to affect strongly the plastic flow of silica glass (e.g., Donnadieu, 1988).

Evidence of the difference in flow properties between the two types of samples was visible. The samples that did not develop a new peak appeared heterogeneous above 10 GPa; the boundaries between glass shards were visible up to the 45 GPa. The glass quenched at pressure, however, became homogenous at approximately 5 GPa. We suggest that this difference arises from the lower yield strength (and perhaps viscosity) of the latter glass sample at high pressure. Lower yield strengths may be associated with a structural transition. In this regard, the behavior may be similar to the decrease in yield strength of SiO_2 glass with pressure reported by Meade and Jeanloz (1988). These changes could result from the destabilization and distortion of the SiO_4 tetrahedra, if not from complete changes in Si coordination (Meade and Jeanloz, 1988; Williams and Jeanloz, 1988).

These observations can be explained by a pressure-induced transition between two structural states of the glass. Evidence for structural (or polymorphic) transitions has been reported in other amorphous materials. Mishima et al. (1985) documented the transition with first-order character between high- and low-density amorphous ice. The hysteresis observed in the glass B samples suggests a transition with first-order character. The transition may also be similar to the changes in structure of SiO_2 glass observed in situ at high pressure beginning at 9 GPa (Hemley et al., 1986; see also Grimsditch, 1984). However, the transition in SiO_2 appears to be associated with a continuum of high-density states, and the high-pressure state can be partially quenched or recovered at room temperature (irreversible compaction), in contrast to the behavior of glass B.

Cation coordination changes

It is useful to examine the evidence for discrete pressure-induced changes in cation coordination in both the Si and alkaline-earth ions. Here we consider both the changes in the high-frequency (tetrahedral Si-O stretching vibrations) as well as the low-frequency bands. Williams and Jeanloz (1988) measured the midinfrared spectrum of $CaMgSi_2O_6$ glass and observed a decrease in absorbance at 1000–1200 cm^{-1} and a concomitant increase at 600–900 cm^{-1} at pressures above 25 GPa; they attributed these changes to a transition from tetrahedral to octahedral Si. Similar changes are observed in infrared spectra of the three glasses studied here. However, the intensities of the high-frequency Raman bands are appreciable up to 45 GPa, and any increase in absorption at 600–900 cm^{-1} is very weak. These results indicate that a significant concentration of SiO_4 groups persists to these pressures, although the tetrahedra may become increasingly distorted with compression of the glass. A small increase in the concentration of more highly coordinated Si could occur, but no peaks were observed in the infrared spectra that may be associated with well-defined $^{[6]}$Si.

Raman spectra measured above 20 GPa for crystalline enstatite, $MgSiO_3$ perovskite, and the two magnesium silicate glasses are shown in Figure 6. The glass spectra are distinct from that of enstatite, which is metastable at these pressures. The Raman spectrum of enstatite shifts continuously with pressures up to at least 30 GPa, which

indicates that the topology of the structure persists over this range at room temperature with no evidence for major structural transitions including amorphization (Hemley, 1987; Hemley et al., 1988). However, small changes in splittings among some of the bands are observed, which are interpreted as evidence of distortions of the low-pressure orthoenstatite structure (Kubicki and Hemley, unpublished data). The stable phase of crystalline $MgSiO_3$ above 24 GPa is orthorhombic perovskite, which has octahedrally coordinated Si (e.g., Yagi et al., 1978; Fei et al., 1989). This phase boundary is close to the pressure at which the 400-cm^{-1} band emerges in the Raman spectra of glass B described above. The high-pressure Raman spectrum of $MgSiO_3$ perovskite has a relatively strong peak in this frequency range. Although such a correlation could suggest that the peak may be characteristic of $^{[6]}$Si, lattice dynamics calculations on $MgSiO_3$ perovskite have shown that Raman-active vibrations in this frequency region (200–400 cm^{-1}) have contributions from translational modes of Mg in the distorted dodecahedral site of the perovskite structure (Hemley et al., 1989b). Hence, the new band in the $MgSiO_3$ glass sample may be associated with Mg ion motions in a high-coordination environment.

Molecular dynamics simulations based on ionic pairwise interatomic potentials were performed to explore further possible structural changes in $MgSiO_3$ glass under pressure. The techniques and details concerning the potentials used are described elsewhere (Kubicki and Lasaga, 1991). The Si and Mg coordinations as a function of density predicted from the MD calculations are listed in Table 1. The MD simulations indicate that the coordination of Mg changes from predominantly tetrahedral at ambient pressure to octahedral at 30 GPa, which corresponds to a volume compression of approximately 20%. The presence of $^{[4]}$Mg at low pressures is supported by the X-ray diffraction study of Yin et al. (1983) and X-ray emission spectra of Hanada et al. (1988). These results indicate that the peak may signal the onset of a $^{[4]}$Mg to $^{[6]}$Mg (or higher) coordination change. If so, the peak may be related to the low-frequency peaks in the $CaSiO_3$ and $CaMgSi_2O_6$ glass spectra due to Ca in octahedral coordination. The proposed increase in Mg coordination with pressure could be coupled to an increase in average Si coordination. The $^{[4]}$Si to $^{[6]}$Si transition may not be apparent in these spectra because the characteristic vibrational modes are weak (e.g., Hemley et al., 1989b), or because of the low concentration of the highly coordinated species, or both. Again, we emphasize that whether such a structural transition occurs at room temperature may be dependent on trace impurities in the glass and the sample history. It is possible that structural transitions in the amorphous material may be kinetically hindered in the compressed glass at room temperature but may become facile at higher temperatures (e.g., above the glass transition), perhaps at lower pressures.

In general, the high-pressure behavior of these glasses at room temperature is thus consistent with a wide range of stability of tetrahedrally coordinated Si. However, it is possible to admit a small concentration of $^{[6]}$Si, perhaps along a continuum of coordination states (e.g., Stolper and Ahrens, 1987). Such a coordination continuum could imply the existence of $^{[5]}$Si as an intermediate species. The Raman and infrared signatures for this species are not yet known, but McMillan et al. (1989) have suggested that Raman intensity at approximately 900 cm^{-1} in spectra of quenched, high-pressure melts may be due to fivefold coordinated Si. This argument is consistent with the increase in Raman intensity with pressure at 900 cm^{-1} in our spectra. Molecular orbital calculations on the $[Si(OH)_5]^{-1}$ molecule predict that $^{[5]}$Si is a stable species with Raman-active Si-OH stretches at 768, 825, and 951 cm^{-1} (Kubicki, 1991). Evidence for the formation of $^{[5]}$Si in glasses quenched at high pressure has been obtained from recent NMR experiments by Stebbins and McMillan (1989). The presence of $^{[5]}$Si in compressed $MgSiO_3$ glass at 300 K is also suggested by the MD simulations (Table 1; see also Kubicki and Lasaga, 1991). MD simulations of the high-temperature melts show that a significant population of $^{[6]}$Si does not form in the melts until very high compressions of $V/V_0 < 0.6$ are reached (Matsui and Kawamura, 1980; Matsui et al., 1981; Kubicki and Lasaga, 1991).

Conclusions

High-pressure Raman and infrared measurements demonstrate that the structures of metasilicate glasses are altered dramatically at pressures above 10 GPa, as observed previously for SiO_2 glass. By far, the predominant changes are reversible; hence, it is necessary to study these glasses in situ in order to obtain information on high-pressure structures and properties. Structural studies of glasses quenched from these pressures give at best an incomplete picture of the effect of compression on the short- and intermediate-range structure of these materials. Comparisons with previous measurements and existing theoretical studies are used to show that the principal compression mechanism at room temperature is the closure of the Si-O-Si angle, at least up to 30 GPa. The loss of diffuse Raman scattering intensity at low frequencies also suggests there is an increase in intermediate range order in these glasses under pressure, as in SiO_2 glass. Increases in cation coordination are inferred from changes in the low-frequency Raman spectra at higher pressures (above ~20 GPa). However, the glasses retain spectral features diagnostic of $^{[4]}$Si up to 45 GPa, although the tetrahedra may be considerably distorted at high compressions. We also present evidence that sample preparation, history, and experimental conditions can have a significant effect on the structural state of the glass spectra under pressure. It remains to be seen whether the structural changes inferred from the present room temperature spectra occur at comparable pressures at higher temperatures (e.g., in high-density melts). These changes may occur at lower pressures as a result of faster kinetics associated with higher O diffusivity, which may also be

enhanced by the compression. Indeed, the variability in high-pressure behavior of glasses with nominally similar compositions may be associated with differences in kinetics for alternative compression mechanisms (i.e., cation coordination) even at room temperature. Direct measurements at high pressure and temperature are required to examine these questions.

Acknowledgments

We thank H.K. Mao, T.C. Hoering, and L.W. Finger for valuable assistance, and F.R. Boyd, H.S. Yoder, and J. Bass for supplying glass samples and for communicating results prior to publication. We also thank C. Meade, R.E. Cohen, A.C. Lasaga, and B.O. Mysen for useful discussions, and P. McMillan, L.E. McNeil, C.T. Prewitt, D.E. Townsend, and L. Stixrude for helpful comments on the manuscript. This work was supported by the National Science Foundation (grant nos. EAR-8418413, EAR-8708192, and EAR-8920239.

References cited

Brandriss, M.E., and Stebbins, J.F. (1988) Effects of temperature on the structures of silicate liquids: NMR results. Geochimica et Cosmochimica Acta, 52, 2659–2669.

Brawer, S.A., and White, W.B. (1977) Raman spectroscopic investigation of the structure of silicate glasses. II. The soda-alkaline earth-alumina ternary and quaternary glasses. Journal of Non-Crystalline Solids, 23, 261–278.

Cohen, A.J., and Gordon, R.G. (1976) Modified electron-gas study of the stability, elastic properties, and high-pressure behavior of MgO and CaO crystals. Physical Review B, 14, 4593–4605.

Cusack, N.E. (1987) The physics of structurally disordered matter, 402 p. Adam Hilger, Philadelphia.

Dickinson, J.E., Scarfe, C.M., and McMillan, P.F. (1990) Physical properties and structure of $K_2Si_4O_9$ melt quenched from pressures up to 2.4 GPa. Journal of Geophysical Research, 95, 15675–15681.

Donnadieu, P. (1988) Influence of impurities on plastic flow of silica glass. Journal of Non-Crystalline Solids, 99, 113–117.

Dowty, E. (1987) Vibrational interactions of tetrahedra in silicate glasses and crystals: I. Calculations on ideal silicate-aluminate-germanate structural units. Physics and Chemistry of Minerals, 14, 80–93.

Eckersley, M.C., Gaskell, P.H., Barnes, A.C., and Chieux, P. (1988a) Structural ordering in a calcium silicate glass. Nature, 335, 525–527.

——— (1988b) The environment of Ca ions in silicate glasses. Journal of Non-Crystalline Solids, 106, 132–136.

Etchepare, J. (1972) Study by Raman spectroscopy of crystalline and glassy diopside. In R.W. Douglas and B. Ellis, Eds., Amorphous materials, papers presented to the International Conference on the Physics of Non-crystalline Solids, p. 337–346. Wiley-Interscience, New York.

Fei, Y., Saxena, S.K., and Navrotsky, A. (1989) Internally consistent thermodynamic data and equilibrium phase relations for compounds in the system MgO-SiO_2 at high pressure and high temperature. Journal of Geophysical Research, 95, 6915–6928.

Fratello, V.J., Hays, J.F., and Turnbull, D. (1981) Dependence of growth rate of quartz in fused silica on pressure and impurity content. Journal of Applied Physics, 51, 4718–4728.

Furukawa, T., Fox, K.E., and White, W.B. (1981) Raman spectroscopic investigation of the structure of silicate glasses. III. Raman intensities and structural units in sodium silicate glasses. Journal of Chemical Physics, 75, 3226–3237.

Galeener, F.L., and Geissberger, A.E. (1983) Vibrational dynamics in ^{30}Si-substituted vitreous SiO_2. Physical Review B, 27, 6199–6204.

Grimsditch, M. (1984) Polymorphism in amorphous SiO_2. Physical Review Letters, 52, 2379–2381.

——— (1986) Annealing and relaxation in the high-pressure phase of amorphous SiO_2. Physical Review B, 34, 4372–4373.

Hanada, T., Soga, N., and Tachibana, T. (1988) Coordination state of magnesium ions in rf sputtered amorphous films in the system MgO-SiO_2. Journal of Non-Crystalline Solids, 105, 39–44.

Hazen, R.M., and Finger, L.W. (1982) Comparative crystal chemistry, 231 p. Wiley-Interscience, New York.

Hazen, R.M., Finger, L.W., Hemley, R.J., and Mao, H.K. (1989) High-pressure crystal chemistry and amorphization of α-quartz. Solid State Communications, 72, 507–511.

Heinz, D.L., and Jeanloz, R. (1987) Measurement of the melting curve of $Mg_{0.9}Fe_{0.1}SiO_3$ at lower mantle conditions and its geophysical implications. Journal of Geophysical Research, 92, 11437–11444.

Hemley, R.J. (1987) Pressure dependence of Raman spectra of SiO_2 polymorphs: α-quartz, coesite, and stishovite. In M.H. Manghnani and Y. Syono, Eds., High-pressure research in mineral physics, p. 347–359. Terra Scientific, Tokyo, and American Geophysical Union, Washington, DC.

Hemley, R.J., and Kubicki, J.D. (1991) Deep mantle melting. Nature, 349, 283–284.

Hemley, R.J., Mao, H.K., Bell, P.M., and Mysen, B.O. (1986) Raman spectroscopy of SiO_2 glass at high pressure. Physical Review Letters, 57, 747–750.

Hemley, R.J., Bell, P.M., and Mao, H.K. (1987) Laser techniques in high-pressure geophysics. Science, 237, 605–612.

Hemley, R.J., Jephcoat, A.P., Mao, H.K., Ming, L.C., and Manghnani, M.H. (1988) Pressure-induced amorphization of crystalline silica. Nature, 334, 52–54.

Hemley, R.J., Chen, L.C., and Mao, H.K. (1989a) New transformations between crystalline and amorphous ice. Nature, 388, 638–640.

Hemley, R.J., Cohen, R.E., Yeganeh-Haeri, A., Mao, H.K., Weidner, D.J., and Ito, E. (1989b) Raman spectroscopy and lattice dynamics of $MgSiO_3$-perovskite at high pressure. In A. Navrotsky and D.J. Weidner, Eds., Perovskite: A structure of great interest to geophysics and materials science, p. 35–44. American Geophysical Union, Washington, DC.

Hibben, J.H. (1935) Raman spectra in inorganic chemistry, Chemical Reviews, 13, 345–478.

Hofmeister, A.M., Xu, J., Mao, H.K., Bell, P.M., and Hoering, T.C. (1989) Thermodynamics of Fe-Mg olivines at mantle pressures: Mid- and far-infrared spectroscopy at high pressure. American Mineralogist, 74, 281–306.

Jayaraman, A. (1983) Diamond-anvil cell and high-pressure physical investigations. Reviews of Modern Physics, 55, 65–108.

Knittle, E., and Jeanloz, R. (1989) Melting curve of $(Mg,Fe)SiO_3$ perovskite to 96 GPa: Evidence for a structural transition in lower mantle melts. Geophysical Research Letters, 16, 421–424.

Kubicki, J.D. (1991) Molecular orbital calculations of transitions between coordination states of $Si(OH)_n$ molecules. Eos, 72, 144.

Kubicki, J.D., and Hemley, R.J. (1988) In situ high-pressure Raman spectra of silicate glasses. Annual Report of Director of the Geophysical Laboratory, 1987–1988, 53–56.

——— (1989) Spectroscopic evidence for a new high-pressure magnesium silicate phase. Annual Report of Director of the Geophysical Laboratory, 1988–1989, 91–94.

Kubicki, J.D., and Lasaga, A.C. (1987) Molecular dynamics simulations of Mg_2SiO_4 and $MgSiO_3$ melts: Structural and diffusivity changes with pressure. Eos, 68, 436.

——— (1991) Molecular dynamics simulation of pressure and temperature effects on $MgSiO_3$ and Mg_2SiO_4 melts and glasses. Physics and Chemistry of Minerals, 17, 661–673.

Lasaga, A.C., and Gibbs, G.V. (1987) Applications of quantum mechanical potential surfaces to mineral physics calculations. Physics and Chemistry of Minerals, 14, 107–117.

——— (1988) Quantum mechanical potential surfaces and calculations on minerals and molecular clusters. Physics and Chemistry of Minerals, 16, 29–41.

Levien, L., Prewitt, C.T., and Weidner, D.J. (1980) Structure and elastic properties of quartz at pressure. American Mineralogist, 65, 920–930.

Liu, L.-G. (1975) Post-oxide phases of forsterite and enstatite. Geophysical Research Letters, 2, 417–419.

Liu, L.-G., and Ringwood, A.E. (1975) Synthesis of a perovskite-type polymorph of $CaSiO_3$. Earth and Planetary Science Letters, 28, 209–211.

Mao, H.K. (1989) Static compression of simple molecular systems in the megabar range, In A. Polian, P. Loubeyre, and N. Boccara, Eds., Simple

molecular systems at very high densities, p. 221–236. Plenum Press, New York.

Mao, H.K., Xu, J., and Bell, P.M. (1986) Calibration of the ruby pressure gauge to 800 kbar under quasi-hydrostatic conditions. Journal of Geophysical Research, 91, 4673–4676.

Mao, H.K., Chen, L.C., Hemley, R.J., Jephcoat, A.P., Wu, Y., and Bassett, W.A. (1989) Stability and equation of state of $CaSiO_3$-perovskite to 134 GPa. Journal of Geophysical Research, 94, 17889–17894.

Matson, D.W., Sharma, S.K., and Philpotts, J.A. (1983) The structure of high-silica alkali-silicate glasses. A Raman spectroscopic investigation. Journal of Non-Crystalline Solids, 58, 323–352.

Matsui, Y., and Kawamura, K. (1980) Instantaneous structure of an $MgSiO_3$ melt simulated by molecular dynamics. Nature, 285, 648–649.

Matsui, Y., Kawamura, K., and Syono, Y. (1981) Molecular dynamics calculations applied to silicate systems: Molten and vitreous $MgSiO_3$ and Mg_2SiO_4. In S. Akimoto and M.H. Manghnani, Eds., High pressure research in geophysics, advances in earth and planetary science, vol. 12, p. 511–524. Reidel, Boston.

McMillan, P. (1984a) A Raman spectroscopic study of glasses in the system CaO-MgO-SiO_2. American Mineralogist, 69, 645–659.

——— (1984b) Structural studies of silicate glasses and melts—applications and limitations of Raman spectroscopy. American Mineralogist, 69, 622–644.

——— (1989) Raman spectroscopy in mineralogy and geochemistry. Annual Reviews in Earth and Planetary Sciences, 17, 255–283.

McMillan, P., Piriou, B., and Couty, R. (1984) A Raman study of pressure-densified vitreous silica. Journal of Chemical Physics, 81, 4234–4236.

McMillan, P., Xue, X., Kanzaki, M., and Stebbins, J.F. (1989) Structural changes in quenched alkali silicate liquids at high pressure: Raman spectroscopy. Eos, 70, 1374.

Meade, C., and Jeanloz, R. (1988) Effect of a coordination change on the strength of amorphous SiO_2. Science, 241, 1072–1073.

Mishima, O., Calvert, L.D., and Whalley, E. (1985) An apparently first-order transition between two amorphous phases of ice induced by pressure. Nature, 314, 76–78.

Moenke, H.H.W. (1974) Silica, the three-dimensional silicates, borosilicates, and beryllium silicates. In V.C. Farmer, Ed., The infrared spectra of minerals, monograph no. 4, p. 383–423. Mineralogical Society of London, London.

Mysen, B.O., Virgo, D., and Scarfe, C.M. (1980) Relations between the anionic structure and viscosity of silicate melts—a Raman spectroscopic study. American Mineralogist, 65, 690–710.

Mysen, B.O., Virgo, D., and Seifert, F.A. (1982) The structure of silicate melts: Implications for chemical and physical properties of natural magma. Reviews of Geophysics and Space Physics, 20, 353–383.

Navrotsky, A., Geisinger, K.L., McMillan, P., and Gibbs, G.V. (1985) The tetrahedral framework in glasses and melts—Inferences from molecular orbital calculations and implications for structure, thermodynamics, and physical properties. Physics and Chemistry of Minerals, 11, 284–298.

Richet, P., and Bottinga, Y. (1986) Thermochemical properties of silicate glasses and liquids: A review. Reviews of Geophysics, 24, 1–25.

Rigden, S.M., Ahrens, T.J., and Stolper, E.M. (1984) Densities of liquid silicates at high pressures. Science, 226, 1071–1074.

——— (1988) Shock compression of molten silicate: Results for a model basaltic composition. Journal of Geophysical Research, 93, 367–382.

Seifert, F.A., Mysen, B.O., and Virgo, D. (1983) Raman study of densified vitreous silica. Physics and Chemistry of Glasses, 24, 141–145.

Sharma, S.K., Mammone, J.F., and Nicol, M.F. (1981) Raman investigations of ring configurations in vitreous silica. Nature, 292, 140–141.

Stebbins, J.F., and McMillan, P.F. (1989) Five- and six-coordinated Si in $K_2Si_4O_9$ glass quenched from 1.9 GPa and 1200 °C. American Mineralogist, 74, 965–968.

Stolper, E.M., and Ahrens, T.J. (1987) On the nature of pressure-induced coordination changes in silicate melts and glasses. Geophysical Research Letters, 14, 1231–1233.

Sweet, J.R., and White, W.B. (1969) Study of sodium silicate glasses and liquids by reflectance spectroscopy. Physics and Chemistry of Glasses, 10, 246–251.

Velde, B., and Couty, R. (1987) High-pressure infrared spectra of some silicate glasses. Chemical Geology, 62, 35–41.

Waff, H.S. (1975) Pressure-induced coordination changes in magmatic liquids. Geophysical Research Letters, 2, 193–196.

Walrafen, G.E., and Krishnan, P.N. (1981) Raman spectrum of pressure compacted fused silica. Journal of Chemical Physics, 74, 5328–5330.

Waseda, Y., and Toguri, J.M. (1977) The structure of molten binary silicate systems CaO-SiO_2 and MgO-SiO_2. Metallurgical Transactions, 8B, 563–568.

Williams, Q., and Jeanloz, R. (1988) Spectroscopic evidence for pressure-induced coordination changes in silicate glasses and melts. Science, 239, 902–905.

Wolf, G.H., Durben, D.J., and McMillan, P.F. (1990) High-pressure Raman spectroscopic study of sodium tetrasilicate ($Na_2Si_4O_9$) glass. Journal of Chemical Physics, 93, 2280–2288.

Wong, J., and Angell, C.A. (1976) Glass structure by spectroscopy, 864 p. Marcel Dekker, Inc., New York.

Xue, X., Stebbins, J.F., Kanzaki, M., and Tronnes, R.G. (1989) Silicon coordination and speciation changes in a silicate liquid at high pressures. Science, 245, 962–964.

Yagi, T., Mao, H.K., and Bell, P.M. (1978) Structure and crystal chemistry of perovskite-type $MgSiO_3$. Physics and Chemistry of Minerals, 3, 97–110.

Yin, C.D., Okuno, M., Morikawa, H., and Marumo, F. (1983) Structure analysis of $MgSiO_3$ glass. Journal of Non-Crystalline Solids, 55, 131–141.

Yoder, H.S. (1976) Generation of basaltic magma, 265 p. National Academy of Sciences, Washington, DC.

Manuscript received September 17, 1990
Manuscript accepted November 5, 1991